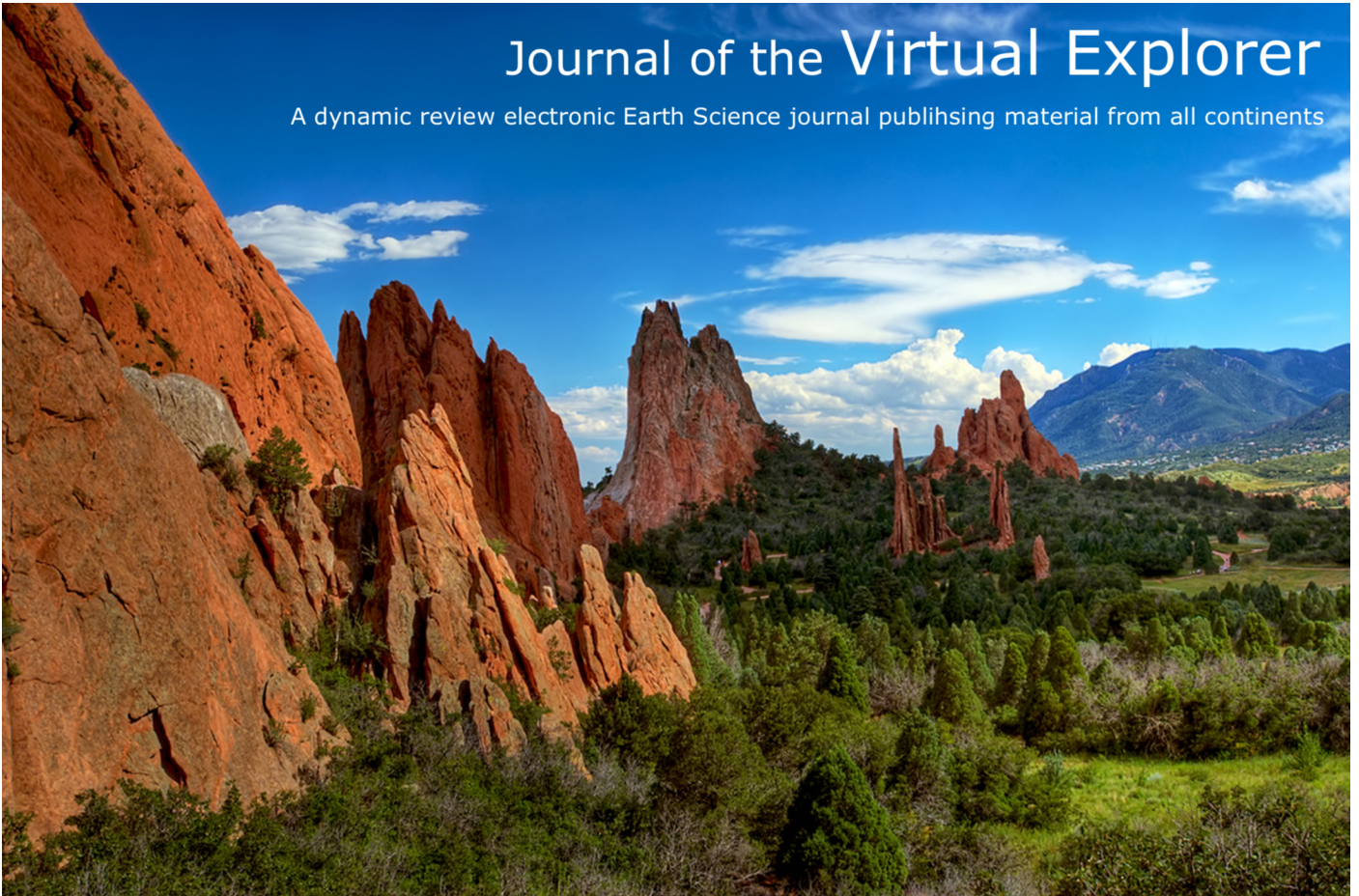


Journal of the Virtual Explorer

A dynamic review electronic Earth Science journal publishing material from all continents



Animation of re-fold structures

Florian Füsseis, Bernhard Grasemann

Journal of the Virtual Explorer, Electronic Edition, ISSN 1441-8142, volume 09, paper 1

In: (Ed.) Andy Bobyarchick,

Visualization, Teaching and Learning in Structural Geology, 2002.

Download from: <http://virtualexplorer.com.au/article/2002/59/animation-of-refold-structures>

Click <http://virtualexplorer.com.au/subscribe/> to subscribe to the Journal of the Virtual Explorer.

Email team@virtualexplorer.com.au to contact a member of the Virtual Explorer team.

Copyright is shared by The Virtual Explorer Pty Ltd with authors of individual contributions. Individual authors may use a single figure and/or a table and/or a brief paragraph or two of text in a subsequent work, provided this work is of a scientific nature, and intended for use in a learned journal, book or other peer reviewed publication. Copies of this article may be made in unlimited numbers for use in a classroom, to further education and science. The Virtual Explorer Pty Ltd is a scientific publisher and intends that appropriate professional standards be met in any of its publications.



Animation of re-fold structures

Florian Füsseis, Bernhard Grasemann

Journal of the Virtual Explorer, Electronic Edition, ISSN 1441-8142, volume **09**, paper 1
In: (Ed.) Andy Bobyarchick, Visualization, Teaching and Learning in Structural Geology, 2002.

Abstract: This work presents computer animations of three-dimensional re-fold structures and their two-dimensional interference patterns, which visualize the complex geometry of simple kinematic fold superposition models. The animations help to improve the understanding of fold interference in both teaching the geometrical background and classifying the enormous variability of natural examples. Because the interference patterns are not indicative for a relative spatial orientation of superposed folds, the re-fold structures are distinguished by the angles between the kinematic axes (i.e. fold axis, the pole to the axial plane and the normal to these axes) of the initial and the superposing fold. These orthogonal triplets of directions can be elegantly plotted in a re-fold-stereoplot, which is simply a stereographic projection where the initial fold axis is oriented W-E and the pole to the axial plane N-S. Six orthogonal, geometrical end-members can be distinguished and used for a classification of all possible superposition geometries, including Type 1-3 after Ramsay (1967). The classical Type 0 end-member re-fold, which in case of perfect cylindrical fold shapes produces no interference patterns, has to be divided in three different classes Type 0₁-0₃. Although these classes are probably difficult to distinguish in the field, Type 0₁-0₃ re-folds result in markedly different distributions of finite strains.

<http://virtualexplorer.com.au/article/2002/59/animation-of-re-fold-structures>

Citation: Füsseis, F., Grasemann, B. 2002. Animation of re-fold structures. In: (Ed.) Andy Bobyarchick, *Journal of the Virtual Explorer*, volume **09**, paper 1, doi: 10.3809/jvirtex.2002.00059

Introduction

Superposition of folding during either progressive displacement or different phases of deformation result in three-dimensional refold structures that are exposed on two-dimensional sections as interference patterns (Ramsay, 1962, 1967). In order to understand the complex geometry of these structures several models have been presented: Earlier models used card decks, which were cut into the shape of the first fold and then sheared parallel to the second fold axial plane (e.g. Carey, 1962, O'Driscoll, 1962, Brown, 1967). Scaled physical models showed the influence of layer buckling, competence contrast between layers and the influence of the initial fold geometry on the formation of refold structures (e.g. Reynolds and Holmes, 1954, Gosh and Ramberg, 1968, Watkinson, 1981, Odonne and Vialon, 1987, Grujic, 1993, Johns and Mosher, 1995). Kinematic forward modelling computer programs have been successfully applied to simulate three-dimensional refolding and to study two-dimensional interference patterns on arbitrary oriented sections through the modelled structures (e.g. Thiessen, 1986, Perrin et al. 1988, Jessell and Valenta, 1996; Vacas Peña, 2000, Ramsay and Lisle, 2000; Moore and Johnson, 2001). Although most of these programs have the same limitations as the card deck models, that folds are assumed to be (cylindrical) similar shear folds with passive initial layering, these studies have significantly contributed to the understanding of the great variety of interference structures and the classification of refolds.

Computer animations of the development of geological structures during progressive deformation are a powerful tool both in the advancement of understanding of processes and geological education. With the help of a computer program for modelling three-dimensional refold structures and their two-dimensional interference patterns, this contribution provides computer animations, which effectively improve the understanding of natural fold superposition and are therefore ideally suited for teaching in electronic classrooms or for use in online courses on the Internet. Furthermore the animations suggest that the Type 0 refold, which actually produces no interference patterns, has to be divided in three different classes, which theoretically exist but which are probably difficult to distinguish in the field. Because the presented study is based on the kinematic forward modelling software Noddy (Jessell and Valenta, 1996) the mechanical influence of contrasting rheologies is ignored and

discussed elsewhere (e.g. Johns and Mosher, 1995 and references cited therein). Despite these limitations the presented results have many geometric similarities with natural refold structures justifying the use of kinematic modelling in exploring the complex shapes and interference patterns of fold superposition (Ramsay and Lisle, 2000).

Mathematical background

The superposition of successive three-dimensional heterogeneous deformations can be expressed by a single Lagrangian equation triplet describing the superposed heterogeneous finite deformation field. This superposition is not commutative and the resulting finite deformation will differ if the order of superposition is reversed.

A deformation, which describes the transformation of an initial coordinate (x, y) to the another coordinate (x_1, y_1) :

$$\begin{aligned} x_1 &= f_a(x, y, z) \\ y_1 &= f_b(x, y, z) \\ z_1 &= f_c(x, y, z) \end{aligned} \quad (1)$$

is superposed by another transformation:

$$\begin{aligned} x_2 &= f_d(x_1, y_1, z_1) \\ y_2 &= f_e(x_1, y_1, z_1) \\ z_2 &= f_f(x_1, y_1, z_1) \end{aligned} \quad (2)$$

deforming (x_1, y_1) to (x_2, y_2) . The total finite displacement field combining Eq. (1) and (2) is given by:

$$\begin{aligned} x_2 &= f_d(f_a(x, y, z), f_b(x, y, z), f_c(x, y, z)) \\ y_2 &= f_e(f_a(x, y, z), f_b(x, y, z), f_c(x, y, z)) \\ z_2 &= f_f(f_a(x, y, z), f_b(x, y, z), f_c(x, y, z)) \end{aligned} \quad (3)$$

By differentiating Eq. (3) it is possible to obtain the nine components of the three-dimensional displacement gradient tensor D in Lagrangian form:

$$D = \begin{pmatrix} \frac{\partial x_2}{\partial x} & \frac{\partial x_2}{\partial y} & \frac{\partial x_2}{\partial z} \\ \frac{\partial y_2}{\partial x} & \frac{\partial y_2}{\partial y} & \frac{\partial y_2}{\partial z} \\ \frac{\partial z_2}{\partial x} & \frac{\partial z_2}{\partial y} & \frac{\partial z_2}{\partial z} \end{pmatrix} \quad (4)$$

Most of the kinematic forward modelling programs use for the functions f in Eq. 1-3 a sinusoid function or Fourier series describing similar folds. Although these

models do not consider layer competence contrasts that might influence the fold geometry by progressive amplification and deamplification of the layers, similar folds are mathematically simple to implement in kinematic models and a good approximation to study the geometry of natural interference structures. A simplest form of a similar fold with a vertical axial surface parallel to the xz coordinate plane with sinusoidal cross-sectional form can be mathematically described by a heterogeneous displacement:

$$\begin{aligned} x_1 &= x \\ y_1 &= y \\ z_1 &= z + a \sin y \end{aligned} \quad (5)$$

where a is the shear amplitude of the fold. Therefore the displacement tensor d in Lagrangian form is:

$$\mathbf{D} = \begin{pmatrix} 1 & 0 & 0 \\ 0 & 1 & 0 \\ 0 & a \cos y & 1 \end{pmatrix} \quad (6)$$

The computer program Noddy (Jessell and Valenta, 1996) uses a more developed mathematical description of

similar-type folds, where the heterogeneous displacement is defined by:

$$\begin{aligned} x_1 &= x \\ y_1 &= y \\ z_1 &= ae^{\frac{-y^2}{c}} f(wz) \end{aligned} \quad (7)$$

Parameter c controls the fold cylindricity and w is the fold wavelength. The displacement tensor d in Lagrangian form is obtained by differentiating Eq. 7:

$$\mathbf{D} = \begin{pmatrix} 1 & 0 & 0 \\ 0 & 1 & 0 \\ 0 & -2e^{-y^2/c} y \sin wz & e^{-y^2/c} \cos wz \end{pmatrix} \quad (8)$$

Any spatial orientation of the modelled fold for subsequent superposition of another fold can be obtained by a displacement tensor R in Lagrangian form defining the rotation around a unit vector v by an angle of α .

$$\mathbf{R} = \begin{pmatrix} \nu_x + (1 - \nu_x^2) \cos \alpha & \nu_x \nu_y (1 - \cos \alpha) + \nu_z \sin \alpha & \nu_x \nu_z (1 - \cos \alpha) - \nu_y \sin \alpha \\ \nu_x \nu_y (1 - \cos \alpha) - \nu_z \sin \alpha & \nu_y + (1 - \nu_y^2) \cos \alpha & \nu_y \nu_z (1 - \cos \alpha) + \nu_x \sin \alpha \\ \nu_x \nu_z (1 - \cos \alpha) + \nu_y \sin \alpha & \nu_y \nu_z (1 - \cos \alpha) - \nu_x \sin \alpha & \nu_z + (1 - \nu_z^2) \cos \alpha \end{pmatrix} \quad (9)$$

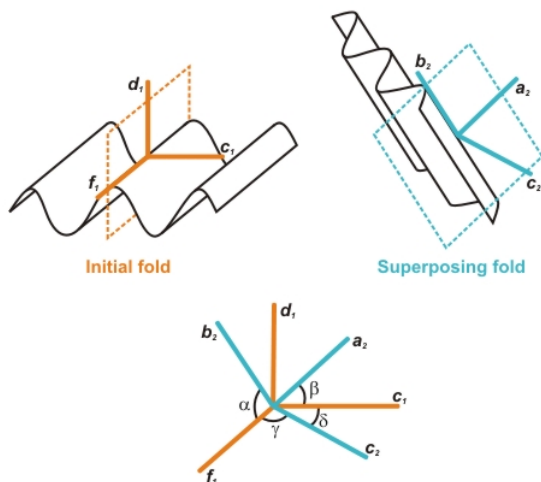
Results can be either displayed by plotting a particular folded and refolded initial surface in three-dimensional space (structure-plot) or by visualizing fold interference patterns on arbitrary cross sections through the structure (pattern-plot).

Classification of re-fold structures

The complex geometries resulting from superposition of folding have been classified by characteristic fold interference patterns, which appear on two-dimensional sections through the three-dimensional re-fold structures (Ramsay, 1967, 1987, Thiessen and Means, 1980, Thiessen, 1986). Ramsay (1967) presented a classification of re-fold structures, which combines two-dimensional interference patterns and three-dimensional superposition geometries, suggesting that individual patterns are indicative for specific spatial angular relationships between the two folding events. These classes (Type 0 - 3) are distinguished by whether the initial fold axes and/or the initial

fold axial planes are deformed during the superposed generation of folding (Fig. 1). The angle between the first (f_1) and second fold axis (b_2) is called a whereas b is the angle between the pole to the first axial plane (c_1) and the second slip or transport direction of heterogeneous displacement (a_2).

Figure 1. Description of kinematic axes of the initial and superposing fold and their relative spatial orientation



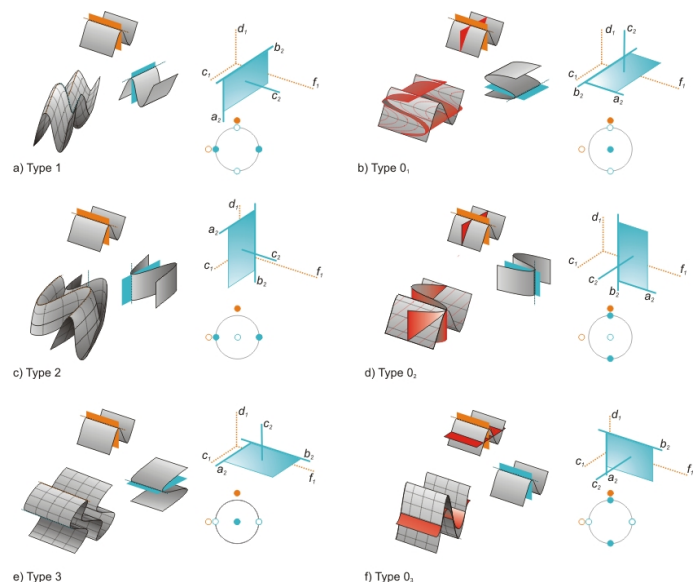
Description of kinematic axes of the initial and superposing fold and their relative spatial orientation (after Ramsay, 1967 and Thiessen and Means, 1980). Initial fold: fold axes = f_1 ; normal to axial plane = c_1 ; direction of heterogeneous shear displacement = d_1 . Superposing fold: fold axes = b_2 ; normal to axial plane = c_2 ; direction of heterogeneous shear displacement = a_2 . Angles between f_1 and b_2 = a ; between c_1 and a_2 = b ; between f_1 and c_2 = g ; between c_1 and c_2 = d .

Using a kinematic modelling computer program Thiessen and Means (1980) introduced g , which is the angle between f_1 and the pole to the second axial plane (c_2), d_1 , which represent the normal to a plane containing c_1 and f_1 , and d , which is the angle between c_1 and c_2 . Various orientations of axes of the first (f_1 , d_1 , c_1) relative to axes of the second fold (b_2 , a_2 , c_2) can be represented by points in a cubic volume with a , b and g plotted along its edges. Because the angles are not independent, not all combinations of a , b and g are possible. Based on this orientation volume diagram and following the terminology of Ramsay (1967), Thiessen and Means (1980) concluded that b and g are appropriate angles for refold classification but that only few interference patterns are really diagnostic for superposition geometries. A single interference pattern can be produced by an infinite number of refold geometries. Furthermore, they concluded that Type 0 refolds do not create in a strict sense interference patterns and that two different geometries of Type 0 refolds exist.

The terminology used in the presented study follows the terminology of Ramsay (1967), which is well established in structural geology textbooks, and extends the

ideas of Thiessen and Means (1980) in following points: (i) The terminology "Type 0-3" is used for end members of three-dimensional refold geometries and not for two-dimensional interference patterns, which have a larger variability (compare fig. 10 in Thiessen, 1986). (ii) Type 0 refolds are further subdivided in three geometrically individual end-members. Because these classes can be simply derived from the refolds Type 1-3 by rotation of the second fold by 90° around the b_2 axis, Type 0 is subdivided in Type 0₁, Type 0₂ and Type 0₃. Directions f_1 , d_1 , c_1 of the initial fold and b_2 , a_2 , c_2 of the superposing fold are called in the following (orthogonal) kinematic axes of the folds (Fig. 1).

Figure 2. Classification of refold structures



Classification of refold structures showing a) Type 1, b) Type 0₁, c) Type 2, d) Type 0₂, e) Type 3 and f) Type 0₃, and corresponding (i) physical orientation of the first and the second fold generation; (ii) resulting, idealized three-dimensional refold structure (iii) orientation of the kinematic axes of the initial and the superposing fold and (iv) stereographic projection of the orientation of the kinematic axes of the initial and the superposing fold (refold-stereoplot).

Figure 2 shows the suggested new classification plotting for each end-member type: (i) The orientation of the first and the second fold generation; (ii) The idealized resulting three-dimensional refold structure; (iii) The orientation of the orthogonal kinematic axes of the first and the second fold generation; (iv) A stereographic projection of the orientation of the kinematic axes of the first and the second fold generation. Concluding, the following six end-member refold types, with an angular

relationship of the initial and superposing kinematic axes of either 0° or 90° can be distinguished:

Type 1 reflow (a and $b = 90^\circ$, $g = 0^\circ$, Fig. 2a): The initial axial plane remains planar, but the fold axes of the superposed fold are deformed. This causes a strong undulation of the hinges of the initial folds resulting in culmination domes and depression basins, where each depression is surrounded by four culminations and each culmination is surrounded by four depressions resembling the shape of an egg-carton. Two-dimensional sections through the reflow structures are often characterized by dome and basin interference patterns (Thiessen, 1986). If $a < 90^\circ$ the domes and basins are arranged en echelon (O'Driscoll, 1962).

Type 2 reflow ($a = 90^\circ$, b and $g = 0^\circ$, Fig. 2c): The initial axial plane and the initial fold axis are deformed. If the reflow structure is progressively unroofed perpendicular to b_2 , interference patterns with circular forms, rounded triangulars, crescent shapes and typical dome-crescent-mushroom patterns characterize the sections (Ramsay and Huber, 1987). However, oblique sections, especially if the reflow structures deviate from the end-member orientation, show a great variability of complex interference patterns (Thiessen, 1986).

Type 3 reflow ($g = 90^\circ$, a , $b = 0^\circ$, Fig. 2e): The initial axial plane is deformed but the initial fold hinges are not bent by superposing folding. Cross sections parallel to the fold axes (f_1 and b_2) will not develop a complex interference pattern but show parallel, straight lines. However, cross sections normal to the fold axes will show complex convergent-divergent or hook shaped interference patterns (Thiessen, 1986).

Type 0 reflow structures always develop when b and $g = 90^\circ$. On two-dimensional sections through the reflow structures no characteristic interference pattern is developed resembling a cross section through a single-phase fold. Although two different end-member geometries of Type 0 refolds have already been noted by Thiessen and Means (1980), these type of reflow structures have attracted little attention of structural geologists mainly because their differences would be difficult to observe in the field. However, if the initial fold generation is cut by a marker plane (e.g. a dyke or vein) at a high angle to f_1 , differences become obvious and three classes have to be distinguished. Note that additionally d , the angle between the normals to the axial planes (c_1 and c_2), is needed for this discrimination (Table 1):

Table 1. Angles between the kinematic axis of the initial and the superposing fold and the corresponding end-members

	$f_1 b_2$	$c_1 a_2$	$f_1 c_2$	$c_1 c_2$
Type 1	90°	90°	0°	90°
Type 0_1	90°	90°	90°	90°
Type 2	90°	0°	0°	90°
Type 0_2	90°	90°	90°	0°
Type 3	0°	0°	90°	90°
Type 0_3	0°	90°	90°	0°

Type 0_1 reflow (a , b , g , $d = 90^\circ$, Fig. 2b): The shearing direction of the superposing fold is parallel to f_1 but axial planes c_1 and c_2 are perpendicular to each other. The resulting reflow structure is identical to the shape of the initial fold. However, a planar passive marker normal to f_1 clearly demonstrates the superposition of heterogeneous deformation. Although cross sections normal to f_1 shows a simple section through a cylindrical fold the deformation is markedly non-plane strain. By rotation of the superposing fold around b_1 , end-member structures Type 1 and Type 0_1 can be continuously transformed into each other (Fig. 4a and b).

Type 0_2 reflow (a , b , $g = 90^\circ$, $d = 0^\circ$, Fig. 2d): The shearing direction of the superposing fold is parallel to f_1 and the axial planes c_1 and c_2 are parallel to each other. The resulting reflow structure is again identical to the shape of the initial fold but a planar passive marker normal to f_1 reveals the superposition of heterogeneous deformation. Again the deformation in a two-dimensional section normal to f_1 is markedly non-plane strain. By rotation of the superposing fold around b_2 , end-member structures Type 2 and Type 0_2 can be continuously transformed into each other (Fig. 5a and b).

Type 0_3 reflow (b , $g = 90^\circ$, a , $d = 0^\circ$, Fig. 2f): Axial planes and fold axes of the initial and the superposing fold are parallel to each other. However, the resulting reflow structure is not identical in shape of the first fold but may be amplified, overprinted or theoretically cancelled. In case of out-of-phase relationship of the waveform of the superposing fold, generation of second order folds on the first fold generation may occur (polyharmonic folds). However, the deformation in a section normal to f_1 is plane strain. This Type 0_3 reflow structure correspond to the Type 0 redundant superposition (Ramsay, 1967;

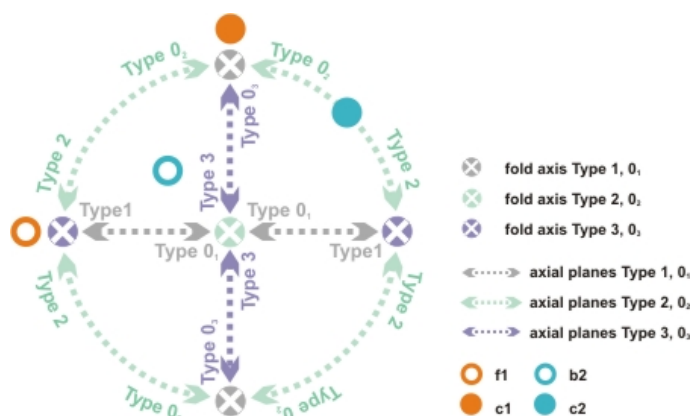
Thiessen and Means, 1980; Ramsay and Huber, 1987). By rotation of the superposing fold around b_2 , end-member structures Type 3 and Type 0_3 can be continuously transformed into each other (Fig. 6a and b).

Animation of refold structures

Animation of refold structures

The animations show finite refold geometries of two folding phases having the same wavelength/amplitude ratio of 2. Two kinds of movies are presented: three-dimensional surface plots (referred to as structure-movies), and fold interference patterns on three perpendicular faces of a block oriented perpendicular to the kinematic axes of the initial fold (referred to as pattern-movies). The animations show the geometrical transition from one refold end-member into another - in 18 steps, with 5° difference each. Note that the orientation of the block models does not change and is identical through all animations. Therefore changes in the shape of the interference patterns result from different superposition geometries and not from changing section orientations. The layers shown in the structure-movies consist of a central layer (dark yellow), visualizing the refold structures, and blue and/or red orthogonal marker layers that were introduced as planes after the first folding event. These marker layers visualize the orientation of the second fold and are therefore crucial for recognizing and distinguishing (!) Type 0_1 , 0_2 and 0_3 refolds. In the pattern-movies refolded marker layers creating interference patterns are shown in dark yellow and pink. Orthogonal marker layers are shown in blue.

Figure 3. Refold-stereoplot



Refold-stereoplot with a fixed orientation of the initial fold having a horizontal W-E striking fold axis and a vertical axial plane with a horizontal pole striking N-S. The c_2 axes of

two different types of end-member refolds plot in the N-S (Type 0_2 and 0_3), W-E (Type 1 and 2) and central position (Type 3 and 0_1) of the refold-stereoplot.

Both the structure- and the pattern-movies additionally show an animated stereographic projection (referred to as refold-stereoplot) of the incremental orientation of the fold axes and axial planes of the initial and superposing fold (Fig. 3). In this refold-stereoplot the spatial orientation of the initial fold is always fixed: f_1 is oriented horizontally W-E and the axial plane is vertical striking W-E with a pole c_1 oriented horizontally N-S. Because the re-fold Types 1-3 can be transformed in their Types 0_1 - 0_3 counterparts by simply rotating their axial plane around the superposing fold axis b_2 this transformation between the end-member positions can be elegantly displayed by traces of c_2 during rotation along either the periphery or along the N-S and W-E diameter of the refold-stereoplot (strictly speaking traces of c_2 during rotation plot along small circles around b_2 for any spatial orientation of the superposing fold):

(i) Type 1 refolds plot in the periphery (fold axis N and S, c_2 E and W) and are transformed to Type 0_1 refolds by translating c_2 along the W-E diameter towards the centre of the refold-stereoplot. (ii) Type 2 fold axes plot in the centre of the diagram, c_2 in the E and W. The refolds are transformed to Type 0_2 refolds by moving c_2 along the periphery of the refold-stereoplot in a N-S orientation. (iii) Type 3 fold axes plot in the E and W, c_2 plots in the centre of the diagram. The refolds are transformed into Type 0_3 refolds by translating c_2 along the N-S diameter towards the periphery of the refold-stereoplot.

Note that although always two different end-member refolds are plotting at the same N-S, W-E or centre node of the refold-stereoplot, the structures are clearly distinguished by the orientation of their fold axis b_2 . The following section gives a short description of the structure- and pattern-movies of all 15 possible combinations of the 6 end-member structures. Although such progressive transitions between the end-member types are purely geometrical we think that a careful study of these animations of developing refold shapes together with the wide range of possible interference patterns is a perfect training for the understanding of complex three-dimensional shapes and intersections occurring in nature. The movies are described in following logical groups:

Table 2. Animation Group 1

From	Into	Structure Movie	Pattern Movie	Rotation
Type 1	Type 0 ₁	Fig 4a	Fig 4b	1
Type 2	Type 0 ₂	Fig 5a	Fig 5b	1
Type 3	Type 0 ₃	Fig 6a	Fig 6b	1

The geometrical difference between the end-members requires rotating c_2 around b_2 by an angle of 90°. Consequently the superposing fold axis does not change its orientation. A natural example of such transitions could be expected in polyphase deformed areas with a great variability in the orientations of the axial plane and a uniform distribution of the fold axis of the superposing folds (e.g. Füsseis, 2001). Note that, despite Type 0₁ - 0₃ do not produce any visible interference patterns, irregular interference patterns can be observed along most of the transition paths. Structures between Type 1 and 0₁ will be characterized by dome-basin and/or pronounced banded s-z-shaped interference patterns, almost resembling an asymmetric crenulation cleavage with microlithons and cleavage domains (e.g. Passchier and Trouw, 1996). These banded s-z-shaped structures are typical and frequently found on two-dimensional sections in polyphase folded areas (Ramsay and Lisle, 2000). Such banded structures also occur on sections through structures between Type 2 and 0₂, where additionally crescent and w/m-shaped intersections are found. Interferences on sections normal to the fold axes from structures between Type 3 and 0₃ are dominated by all variations of hooks and irregular convergent-divergent patterns. Note that this progressive transition between Type 3 and 0₃ is the only model, where sections parallel to the fold axes would always record plane strain deformation.

Table 3. Animation Group 2

From	Into	Structure-Movie	Pattern-Movie	Rotation
Type1	Type2	Fig7a	Fig7b	1
Type1	Type3	Fig8a	Fig8b	2
Type2	Type3	Fig9a	Fig9b	1

These animations show the transitions between the classical end-members of fold interferences (Ramsay,

1967). Shapes like convergent-divergent hooks, dome and basins and dome-crescent-mushrooms patterns can be observed in the movies. However, note the great complexity and variety of the patterns even on sections orthogonal to the kinematic axes of the perfect cylindrical initial folds. Type 1 is transformed in Type 2 by rotation parallel to c_2 and therefore the superposing axial plane does not change its orientation. Similarly the transition from the Type 2 into Type 3 requires a simple rotation around the orientation of c_1 .

Whereas all previous examples could be transformed by a single rotation about one of the kinematic axes of the superposing fold, the transition of Type 1 into Type 3 needs either two kinematic rotation axes, or a single, oblique rotation axis that has to be constructed from the re-fold-stereoplot: (i) Find the great circle containing b_2 of both Type 1 and Type 3 refolds and determine its pole Pb_2 . (ii) Find the bisector of the angle between b_2 of Type 1 and b_2 of Type 3 re-fold. (iii) Draw a great circle between the bisector and Pb_2 (iv) Repeat this construction for c_2 of both Type 1 and Type 3 refolds. (v) The intersections between the great circles containing the bisectors represents the single oblique rotation axis transforming Type 1 into Type 3 re-fold structure.

Table 4. Animation Group 3

From	Into	Structure-Movie	Pattern-Movie	Rotation
Type0 ₁	Type0 ₂	Fig10a	Fig10b	1
Type0 ₁	Type0 ₃	Fig11a	Fig11b	1
Type0 ₂	Type0 ₃	Fig12a	Fig12b	2

This set of animations show the transition between Type 0 re-fold structures and emphasizes the importance of distinguishing between the suggested classes Type 0₁, 0₂ and 0₃.

The transformations from Type 0₁ into 0₂ and Type 0₂ into 0₃ are again controlled by a simple rotation around one of the kinematic axes of the superposing fold (a_2 and c_2 respectively). On sections perpendicular to f_1 no interference patterns are observed, and the sections normal to d_1 and c_2 show simple linear intersections throughout the transformation. However, folding of a marker layer intruded normal to f_1 and/or to d_1 clearly demonstrates the superposed heterogeneous deformation. If this superposition is not recognized, the assumption of plane strain in a

cross section perpendicular to f_1 is wrong and could lead to potential misinterpretations (e.g. when reconstructing balanced cross sections).

The transformation from Type into 0_1 into 0_3 is more complex and was performed using two rotations around a_2 and c_2 . A single oblique rotation axes can be constructed from the refold-stereoplot with the same method outlined above. Although both end-members show no interference patterns on orthogonal sections to the kinematic axes of the initial fold, the transition refolds create a broad spectrum of complex interference shapes, e.g. dome-basins, crescent, s/z, complex hooks and banded structures.

Table 5. Animation Group 4

From	Into	StructureMovie	Pattern-Movie	Rotation
Type 1	Type 0_3	Fig 13a	Fig 13b	1
Type 3	Type 0_1	Fig 14a	Fig 14b	1
Type 1	Type 0_2	Fig 15a	Fig 15b	2
Type 2	Type 0_1	Fig 16a	Fig 16b	2
Type 2	Type 0_3	Fig 17a	Fig 17b	2
Type 3	Type 0_2	Fig 18a	Fig 18b	2

The remaining six transformations between end-members describe transitions from Type 1, 2 and 3 refolds to Type 0 classes excluding the simple rotations around b_2 already described. The Type 1 into Type 0_3 transformation results from a single rotation around the a_2 axis. On a section perpendicular to this rotation axis regular dome-basin interference patterns (egg-carton structures) are progressively converted in en-echelon basin and domes (O'Driscoll, 1962) until all refolds are cylindrical with parallel fold axes resulting in linear intersection on planes perpendicular to d_1 and c_1 respectively. The Type 3 into Type 0_1 transformation is again based on a single rotation but contrary to the previous example around the c_2 axis. On sections perpendicular to the f_1 axis hooks are progressively "unfolded" and similar to the previous model result in cylindrical refolds with parallel fold axes and consequently in linear intersections on planes perpendicular to d_1 and c_1 .

The following transformations are more complex and require rotations of the superposing folds around oblique

axis or again, as they were modelled for the movies shown, around two, orthogonal axes:

The transition from Type 1 into Type 0_2 shows on the section normal to d_1 changeovers from dome-basins into asymmetric mushroom shapes and banded s/z structures. Interference patterns on sections normal to c_1 reveal an interesting succession from unfolding, asymmetric folding and again unfolding to linear intersection. The symmetric fold intersections on the section normal to f_1 transform into dome-basins, which get progressively overprinted with hooks showing again symmetric folds after complete transformation into Type 0_2 refolds.

The interference patterns on three sections perpendicular to the kinematic axes of the initial fold between the end-members Type 2 and Type 0_1 are characterized by symmetric crescent mushrooms shapes normal to d_1 , hooks normal to f_1 and banded s/z and w/m shapes normal to c_1 .

Whereas the interference patterns on two orthogonal sections of the transformation model between Type 2 and Type 0_3 are very similar to patterns discussed in the previous two models, showing asymmetric mushroom shapes and banded s/z structures, the section perpendicular to f_1 is striking complicated: banded structures reveal multifaceted changes in irregular hook shaped folds.

The transformation of Type 3 into Type 0_2 creates rather similar interference patterns than Type 3 into Type 0_1 or Type 0_3 : Hook-shapes of the convergent divergent patterns on sections normal to f_1 are progressively "unfolded" resulting in a sinusoidal intersections in the Type 0 end-members, but on other orthogonal sections only straight intersections can be observed. However, careful inspections of the movies reveal the distinct differences emphasizing the need to distinguish between Type 0_1 , 0_2 and 0_3 . Even more important is the fact that only the transition into the Type 0_3 end-member is plane strain and all other sections normal to f_1 are markedly non-plane strain.

Given the striking complexity of interference patterns and their continuous transitions between the end-member refold structures, this short description of the movies is far from being complete. It is left to the reader to explore the great variability of interference patterns and to compare the results of the animations with shapes suggested by Thiessen (1986). It is very instructive to observe the development of the blue and red marker planes introduced to the models after the initial folding especially when Type 0 end-members are modelled. Without this

marker planes it is impossible to distinguish between Type 0₁, 0₂ and 0₃.

Conclusions

1) Although limited by a number of simplifications and assumptions, kinematic forward modelling of re-fold structures is a powerful tool in teaching, learning and exploring the enormous complexity and variability of interference patterns. Especially the presented animations help to understand the transitions of complex three-dimensional geometries (structure-movies) and their intersections on planar orthogonal faces (pattern-movies).

2) As already suggested in previous works, the interference patterns are not indicative for a relative spatial orientation of superposed folds. Therefore re-fold structures are distinguished by their three-dimensional geometry described by the angles between the kinematic axes of the initial and superposing fold. These kinematic axes, which are defined as an orthogonal triplet of directions corresponding to the fold axis, the pole to the axial plane and the normal to these axes, can be plotted in a re-fold-stereoplot, which is simply a stereographic projection where the initial fold axis is oriented W-E and the pole to the axial plane N-S.

3) Although Type 0 re-fold structures have been previously described their importance and their classification

in three different end-members have been mainly ignored. Although Type 0 refolds fail to produce interference patterns on sections perpendicular to the kinematic axes of the initial fold, kinematic modelling shows by means of orthogonal marker planes established after initial folding, that the three Type 0 end-members are markedly different. Slight deviations of the end-member geometries result in complex interference patterns, which are considerable different for the three Type 0 end-members. Importantly only the 'classical' Type 0 re-fold structures is plane strain and sections perpendicular to the fold axis of the initial fold are clearly non-plane strain for the two other Type 0 refolds.

4) Therefore we suggest to distinguish Type 1, Type 2, Type 3, Type 0₁, 0₂ and 0₃ re-fold structures.

Acknowledgements

Many thanks to Ulli Exner, Esther Hintersberger, Mark Handy, Mark Jessell, Neil Mancktelow, Hugh Rice, Helmuth Sülva and Gerhard Wiesmayr for fruitful discussions. This work was supported by the Austrian Hochschuljubiläumsstiftung der Stadt Wien (Project Nr. 166/2000) and the FWF Fonds zur Förderung der wissenschaftlichen Forschung (Project Nr. P13227 and P-14129-GEO).

References

- Brown, S. P. 1967. Anatomy of a refold - an empirical approach. *Empire State Geogram* 5, 9-14.
- Carey, W. S. 1962. Folding. *J. Alberta Soc. Pet. Geol.* 10, 95-144.
- Fusseis, F. 2001. The eo-Alpine high-pressure rocks of the Schobergruppe, Austria - Exhumation related deformation. Diplom Thesis, University of Vienna.
- Gosh, S. K. and Ramberg, H. 1968. Buckling experiments on intersecting fold patterns. *Tectonophysics* 5, 89-105.
- Grujic, D. 1993. The initial influence of initial fold geometry on Type 1 and Type 2 interference patterns: an experimental approach. *Journal of Structural Geology* 15/3-5, 293-307.
- Jessell, M. W. and Valenta, K. 1996. Structural Geophysics: Integrated structural and geophysical modeling. In: De Paor, D. G (Ed.). *Structural Geology and Personal Computers, Computer Methods in the Geosciences* 13, 303-324.
- Johns, M. K. and Mosher, S. 1995. Physical models of regional fold superposition: the role of competence contrast. *Journal of Structural Geology* 18/4, 475-492.
- Moore, R. R. and Johnson, S. E. 2001. Three-dimensional reconstruction and modelling of complexly folded surfaces using Mathematica. *Computers and Geosciences* 27/4, 401-418.
- Odonne, F. and Vialon, P. 1987. Hinge migration as a mechanism of superimposed folding. *Journal of Structural Geology* 9, 835-844.
- O'Driscoll, E. S. 1962. Experimental patterns in superimposed similar folding. *J. Alberta Soc. Pet. Geol.* 10, 145-167.
- Passchier, C. W. and Trouw, R. A. J. 1996. *Microtectonics*. Berlin - Heidelberg - New York. 289 p.
- Perrin, M., Oltra, P. H. and Coquillart, S. 1988. Progress in the study and modelling of similar fold interferences. *Journal of Structural Geology* 10/6, 593-605.
- Ramsay, J. G. 1962. Interference patterns produced by the superposition of folds of similar types. *Journal of Geology* 70, 466-481.
- Ramsay, J.G., 1967. *Folding and Fracturing of Rocks*. New York - London. 568 p.
- Ramsay, J. G. and Huber, I. M. 1987. *The Techniques of Modern Structural Geology. Volume 2: Folds and Fractures*. London - San Diego. 309-700 p.
- Ramsay, J. G. and Lisle, R. J. 2000. *The Techniques of Modern Structural Geology. Volume 3: Applications of Continuum Mechanics in Structural Geology*. London - San Diego. 701-1061 p.
- Reynolds, D. L. and Holmes, A. 1954. The superposition of Caledonoid folds on the older fold-system in the Dalradians of Malin Head, Co. Donegal. *Geological Magazine* 91, 417-433.
- Thiessen, R. L. 1986. Two-dimensional refold interference patterns. *Journal of Structural Geology* 8/5, 563-573.
- Thiessen, R. L. and Means W. D. 1980. Classification of fold interference patterns: a re-examination. *Journal of Structural Geology* 2, 311-326.
- Vacas Peña, J. M. 2000. A program in Pascal to simulate the superposition of two or three fold systems. *Computers And Geosciences* 26/3, 341-349.
- Watkinson, A. J. 1981. Patterns of fold interference: influence of early fold shapes. *Journal of Structural Geology* 3, 19-23.